



## Erratum: "Linear and second-order nonlinear optical properties of ionic organic crystals" [J. Chem. Phys. 141, 104109 (2014)]

Tomasz Seidler, Katarzyna Stadnicka, and Benoît Champagne

Citation: *The Journal of Chemical Physics* **142**, 239901 (2015); doi: 10.1063/1.4922617

View online: <http://dx.doi.org/10.1063/1.4922617>

View Table of Contents: <http://scitation.aip.org/content/aip/journal/jcp/142/23?ver=pdfcov>

Published by the [AIP Publishing](http://aip.org)

---

### Articles you may be interested in

[CH<sub>3</sub>OH...n\(H<sub>2</sub>O\) n \[n = 1-4\] clusters in external electric fields](#)

*J. Chem. Phys.* **142**, 214309 (2015); 10.1063/1.4921380

[Investigation of the linear and second-order nonlinear optical properties of molecular crystals within the local field theory](#)

*J. Chem. Phys.* **139**, 114105 (2013); 10.1063/1.4819769

[Chemical verification of variational second-order density matrix based potential energy surfaces for the N 2 isoelectronic series](#)

*J. Chem. Phys.* **132**, 114112 (2010); 10.1063/1.3354910

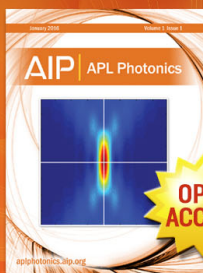
[Energy of charged states in the acetanilide crystal: Trapping of charge-transfer states at vacancies as a possible mechanism for optical damage](#)

*J. Chem. Phys.* **120**, 7095 (2004); 10.1063/1.1669376

[Theoretical study of the second-order nonlinear optical properties of \[N\]helicenes and \[N\]phenylenes](#)

*J. Chem. Phys.* **120**, 2042 (2004); 10.1063/1.1635353

---



Launching in 2016!

The future of applied photonics research is here

OPEN  
ACCESS

AIP | APL  
Photonics

## Erratum: “Linear and second-order nonlinear optical properties of ionic organic crystals” [J. Chem. Phys. 141, 104109 (2014)]

Tomasz Seidler,<sup>1,2,a)</sup> Katarzyna Stadnicka,<sup>1</sup> and Benoît Champagne<sup>2,b)</sup>

<sup>1</sup>Faculty of Chemistry, Jagiellonian University, ul. Ingardena 3, 30-060 Kraków, Poland

<sup>2</sup>Laboratoire de Chimie Théorique, University of Namur, Rue de Bruxelles, 61, B-5000 Namur, Belgium

(Received 16 April 2015; accepted 4 June 2015; published online 15 June 2015)

[<http://dx.doi.org/10.1063/1.4922617>]

In that paper, the linear [ $\chi^{(1)}$ ] and second-order nonlinear [ $\chi^{(2)}$ ] optical properties of three ionic organic crystals, 4-*N,N*-dimethylamino-4'-*N'*-methyl-stilbazolium tosylate (DAST), 4-*N,N*-dimethylamino-4'-*N'*-methyl-stilbazolium 2,4,6-trimethylbenzenesulfonate (DSTMS), and 4-*N,N*-dimethylamino-4'-*N'*-phenyl-stilbazolium hexafluorophosphate (DAPSH), have been calculated by adopting a two-step multi-scale procedure, which consists in calculating (i) the dressed ion properties using point charges for describing the inhomogeneous polarizing field, and then (ii) in accounting for the crystal local field effects using classical electrostatic models. For comparison, results obtained by using a homogeneous dipole field have also been provided for DAST. Though the results obtained by considering the cation/anion pairs are correct and lead to conclude that the dipole field procedure presents severe drawbacks, those reported by considering separately the dressed properties of the cation and anion are incorrect. This originates from a mistake in calculating the ion *dipole moments*, as needed to evaluate the electric field [Eq. (5) of Ref. 1]. Here, we report the corrected values for DAST as well as the values for DSTMS and DAPSH, we interpret these data and assess the reliability of the dipole field approach for ionic organic crystals.

The corrected dipole moments together with the components of the electric field vector are reported in Table I for the three systems. The procedure used to calculate the dipole electric field, summarized in Refs. 1 and 2, converged to 0.05 GV/m in 3, 2 and 1 cycles for DAST, DSTMS, and DAPSH, respectively. First the dipole field is evaluated at the B3LYP/6-311++G(d,p) level of approximation, so are the dressed polarizabilities and first hyperpolarizabilities. In a second step, using the same B3LYP dipole field, the dressed polarizabilities and first hyperpolarizabilities are evaluated at the second-order Møller-Plesset perturbation theory (MP2) level. In the case of dynamic MP2 results, the dressed properties were obtained using the same approach as in Ref. 3, i.e., by scaling the MP2 static molecular properties by the ratio between the dynamic and static B3LYP responses. It is reminded that the dipole moments are calculated at the barycenters of the nuclear charges, which is an easy way to overcome the origin-dependency problem of the dipole moment of a charged molecule but does not preclude from questioning its reliability for computing the linear and nonlinear optical properties.

The resulting polarizing electric field and vectorial hyperpolarizability ( $\lambda = \infty$ ) obtained for DAST cation are depicted in Figure 1. Similarly to the charge field, the dipole electric field damps the hyperpolarizability of the cation. The values of the calculated dipole moments and resulting electric field at the cationic and anionic sites are provided in Table I. A comparison

TABLE I. Cation and anion dipole moments (in D) and electric field (in GV/m) in the abc\* (orthogonal) reference frame obtained at the B3LYP/6-311++G(d,p) level of approximation.

		Cycle	$\mu_x$	$\mu_y$	$\mu_z$	$ \mu $	$F_x$	$F_y$	$F_z$	$ E $
DAST	Cation	0th	-7.05	-2.44	0.45	7.48	-1.87	-0.05	0.32	1.90
		3rd	-11.82	-3.80	1.07	12.46	-1.76	-0.04	0.33	1.79
	Anion	0th	-11.34	0.90	0.85	11.41	-4.35	0.18	0.43	4.37
		3rd	-14.72	1.09	0.85	14.80	-4.28	0.21	0.40	4.31
DSTMS	Cation	0th	-6.87	-2.95	0.31	7.48	-1.41	-0.45	0.65	1.62
		2nd	-10.89	-4.44	1.05	11.80	-1.34	-0.43	0.65	1.55
	Anion	0th	-10.24	-0.38	1.05	10.30	-4.40	0.00	0.40	4.41
		2nd	-14.17	-0.40	1.41	14.24	-4.37	-0.01	0.39	4.39
DAPSH	Cation	0th	-1.11	-0.56	0.25	1.26	-0.16	0.07	-0.18	0.25
		1st	-1.55	-0.70	0.23	1.71	-0.16	0.07	-0.18	0.25
	Anion	0th	0.03	0.20	0.01	0.20	-0.17	0.15	0.00	0.23
		1st	0.01	0.22	0.01	0.22	-0.17	0.15	0.00	0.23

<sup>a)</sup>tomasz.seidler@unamur.be

<sup>b)</sup>benoit.champagne@unamur.be

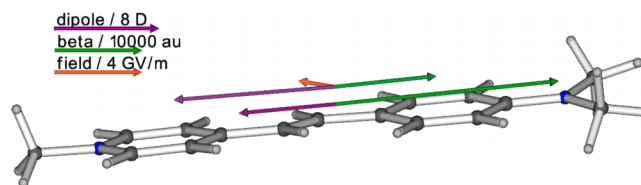


FIG. 1. Calculated dipole moment, vectorial first hyperpolarizability ( $\lambda = \infty$ ), and dipole field for the DAST cation (lower vectors—no field, upper vectors—with inclusion of the converged dipole field).

TABLE II. Static  $\chi^{(1)}$  and  $\chi^{(2)}$  values as obtained from molecular properties evaluated at the B3LYP/6-311++G(d,p) level using the dipole polarizing electric field with cation and anion treated separately in comparison to the values obtained without dressing field and with the charge field.

	Cycle	$\chi_{11}^{(1)}$	$\chi_{22}^{(1)}$	$\chi_{33}^{(1)}$	$\chi_{13}^{(1)}$	$\chi_{111}^{(2)}$	$\chi_{122}^{(2)}$
DAST	Expt.	3.303	1.513	1.466	0.175		
	No field	4.209	1.636	1.449	-0.255	281.3	34.4
	Charge field	3.684	1.553	1.443	-0.223	215.2	25.7
	Dipole field	3.641	1.561	1.456	-0.230	197.3	24.2
DSTMS	Expt.	3.098	1.647	1.500	-0.101		
	No field	3.882	1.789	1.480	-0.218	228.6	39.4
	Charge field	3.441	1.683	1.472	-0.200	176.4	30.0
	Dipole field	3.492	1.714	1.487	-0.213	172.5	29.9
DAPSH	Expt.	3.554	1.455	1.415	-0.889		
	No field	4.088	1.729	1.492	-0.896	260.1	18.8
	Charge field	3.753	1.700	1.465	-0.792	239.0	17.3
	Dipole field	4.060	1.727	1.489	-0.888	256.1	18.5

TABLE III. Static  $\chi^{(1)}$  and  $\chi^{(2)}$  values as obtained from molecular properties evaluated at the MP2/6-311++G(d,p) level using the dipole polarizing electric field with cation and anion treated separately in comparison to the values obtained without dressing field and with the charge field.

	Polarizing field	$\chi_{11}^{(1)}$	$\chi_{22}^{(1)}$	$\chi_{33}^{(1)}$	$\chi_{13}^{(1)}$	$\chi_{111}^{(2)}$	$\chi_{122}^{(2)}$
DAST	Expt.	3.303	1.513	1.466	0.175		
	No field	4.231	1.632	1.451	-0.265	565.8	66.6
	Charge field	3.382	1.514	1.442	-0.204	275.5	32.7
	Dipole field	3.356	1.521	1.453	-0.210	263.3	31.8
DSTMS	Expt.	3.098	1.647	1.500	-0.101		
	No field	3.899	1.769	1.475	-0.222	458.4	75.2
	Charge field	3.190	1.625	1.467	-0.188	233.0	38.5
	Dipole field	3.242	1.652	1.479	-0.200	242.2	40.4
DAPSH	Expt.	3.554	1.455	1.415	-0.889		
	No field	4.048	1.726	1.476	-0.886	501.8	46.4
	Charge field	3.487	1.666	1.425	-0.713	343.3	32.2
	Dipole field	3.992	1.721	1.470	-0.869	483.4	44.9

of calculated  $\chi^{(1)}$  and selected  $\chi^{(2)}$  tensor components in the static limit is presented in Tables II and III for B3LYP and MP2 methods, respectively. Dynamic values at  $\lambda = 1907$  nm are provided for the MP2 method in Table IV. Minor corrections were also made to the MP2-based  $\chi^{(1)}$  and  $\chi^{(2)}$  DAPSH values obtained without dressing fields. The wavelength dispersions of the refractive indices are depicted and compared to experiment as well as to the results obtained with the charge field approach in Figures 2 (DAST), 3 (DSTMS), and 4 (DAPSH). In the case of DAST and DSTMS, the  $\chi^{(1)}$  and  $\chi^{(2)}$  values are very close to those obtained with the charge field approach. Similarly, the wavelength dispersion of the refractive indices obtained with the dipole field closely matches the experimental data. The situation is much different for DAPSH. Indeed, the dipole field model leads to macroscopic properties that are much different from those evaluated using the charge field and, to some extent, are similar to those without accounting for dressing field. This leads also for  $n$  to larger deviations with respect to experiment. Moreover, when confronting the  $\chi_{111}^{(2)}$  tensor component of DAPSH to experiment, at  $\lambda = 1907$  nm, the dipole field yields overestimation of ca. 53% with respect to the upper experimental estimate (580 pm/V) (Table IV), whereas the charge field leads to a good agreement. These weak dressing effects are attributed to the small dipole moments of the ions and therefore to the small dressing fields. Choosing the barycenter of nuclear charges as origin is therefore not a universal recipe for calculating

TABLE IV. Dynamic ( $\lambda = 1907$  nm)  $\chi^{(1)}$  and  $\chi^{(2)}$  values as obtained from molecular properties evaluated at the MP2/6-311++G(d,p) level using the dipole polarizing electric field with cation and anion treated separately in comparison to the values obtained without dressing field and with the charge field.

	Polarizing field	$\chi_{11}^{(1)}$	$\chi_{22}^{(1)}$	$\chi_{33}^{(1)}$	$\chi_{13}^{(1)}$	$\chi_{111}^{(2)}$	$\chi_{122}^{(2)}$	$\chi_{212}^{(2)}$
DAST	Expt.	3.440	1.547	1.484	0.193	420(110)	64(8)	50(6)
	No field	4.498	1.699	1.460	-0.288	1095.5	121.5	120.8
	Charge field	3.532	1.537	1.450	-0.217	447.5	52.0	51.9
	Dipole field	3.502	1.543	1.461	-0.223	426.1	50.5	50.4
DSTMS	Expt.	3.220	1.674	1.504	-0.108	428(40)	62(8)	70(8)
	No field	4.130	1.811	1.484	-0.236	875.4	135.7	135.3
	Charge field	3.323	1.651	1.475	-0.197	378.0	60.9	60.9
	Dipole field	3.381	1.680	1.488	-0.210	398.9	64.9	64.9
DAPSH	Expt.	3.726	1.495	1.438	-0.951	580(80)	30(4)	
	No field	4.298	1.763	1.508	-0.960	932.6	84.7	90.1
	Charge field	3.663	1.694	1.450	-0.765	558.1	53.3	54.6
	Dipole field	4.235	1.757	1.501	-0.941	887.6	81.1	85.9

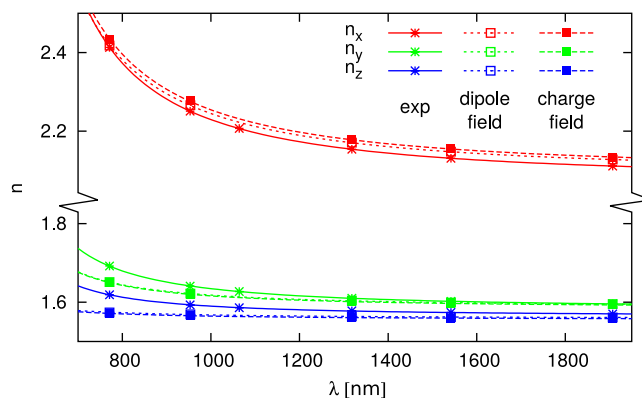


FIG. 2. Wavelength dispersion of refractive indices for DAST obtained with the MP2/6-311++G(d,p) method.

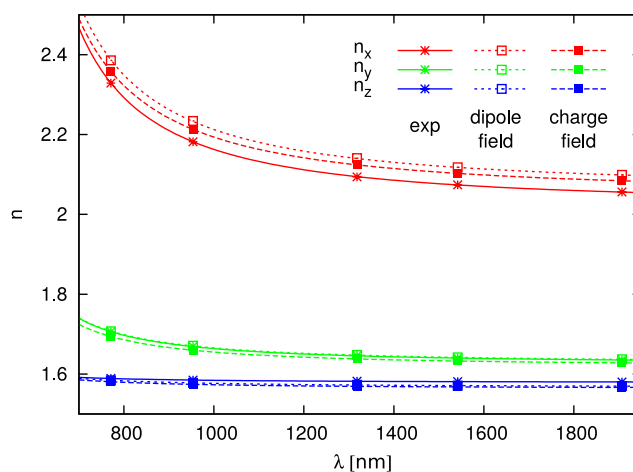


FIG. 3. Wavelength dispersion of refractive indices for DSTMS obtained with the MP2/6-311++G(d,p) method.

the macroscopic optical responses of organic ionic crystals. This is further illustrated by assessing, for DAPSH, the dependence of these different properties as a function of the origin of the axes system for calculating the dipole moment of the cation. Starting from the barycenter of nuclear charges (0), the origin was displaced along the N-N charge transfer direction by 1 Å (p1), 2 Å (p2), -1 Å (m1), and -2 Å (m2). The resulting B3LYP/6-311++G(d,p) results are provided in Table V whereas the effect of the origin shift on the dipole moment and on the dipole field is visualized in Fig. 5. The dipole moment variations induced by the origin shift translate to substantial changes in the dressing field and therefore in the linear and nonlinear optical responses. Among these, some are in close agreement with the charge field results but the choice of the corresponding origin is

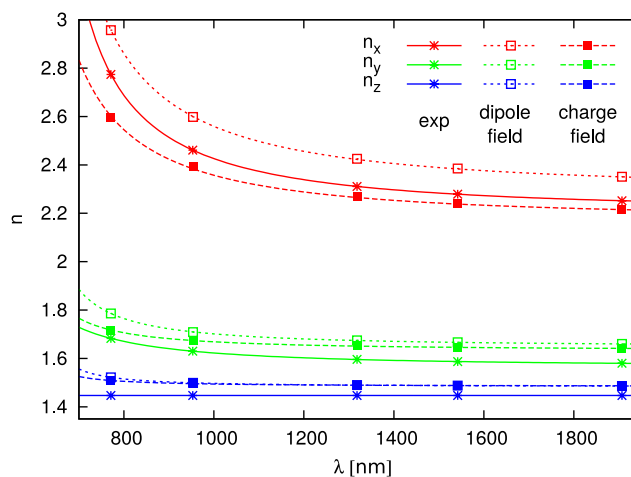


FIG. 4. Wavelength dispersion of refractive indices for DAPSH obtained with the MP2/6-311++G(d,p) method.

TABLE V. Impact of the origin of axes system on the dipole moment of the cation, on the cation dipole field, as well as on the static  $\chi^{(1)}$  and  $\chi^{(2)}$  values for DAPSH as obtained at the B3LYP/6-311++G(d,p) level.

Origin choice	Cycle	$\mu_x$	$\mu_y$	$\mu_z$	$ \mu $	$F_x$	$F_y$	$F_z$	$ E $	$\chi_{11}^{(1)}$	$\chi_{22}^{(1)}$	$\chi_{33}^{(1)}$	$\chi_{13}^{(1)}$	$\chi_{111}^{(2)}$	$\chi_{122}^{(2)}$
"m2"	0th	7.63	1.98	-2.84	8.38	0.77	0.03	-0.03	0.77	4.088	1.729	1.492	-0.896	260.1	18.8
	2nd	10.63	2.62	-3.71	11.56	0.79	0.03	-0.02	0.80	4.338	1.748	1.519	-0.972	294.4	21.3
"m1"	0th	3.26	0.71	-1.30	3.58	0.31	-0.02	-0.10	0.32	4.088	1.729	1.492	-0.896	260.1	18.8
	1st	4.48	0.94	-1.72	4.89	0.31	-0.02	-0.10	0.33	4.195	1.737	1.503	-0.929	275.1	19.9
"0"	0th	-1.11	-0.56	0.25	1.26	-0.16	-0.07	-0.18	0.25	4.088	1.729	1.492	-0.896	260.1	18.8
	1st	-1.54	-0.70	0.23	1.71	-0.16	-0.07	-0.18	0.25	4.060	1.727	1.489	-0.888	256.1	18.5
"p1"	0th	-5.47	-1.83	1.79	6.04	-0.62	-0.12	-0.26	0.69	4.088	1.729	1.492	-0.896	260.1	18.8
	1st	-7.45	-2.31	2.14	8.09	-0.62	-0.12	-0.25	0.68	3.927	1.717	1.475	-0.847	235.5	17.1
"p2"	0th	-9.84	-3.10	3.34	10.84	-1.09	-0.17	-0.33	1.16	4.088	1.729	1.492	-0.896	260.1	18.8
	2nd	-13.24	-3.90	4.02	14.38	-1.06	-0.17	-0.32	1.12	3.805	1.707	1.461	-0.808	213.4	15.4

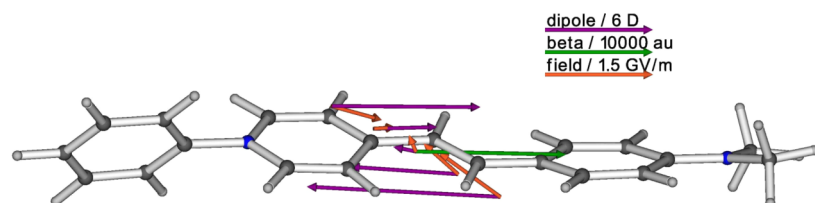


FIG. 5. Impact of the origin on the dipole moment, on the electric field, and on the vectorial first hyperpolarizability ( $\lambda = \infty$ ) for the DAPSH cation (0th cycle values for all quantities). For better readability, the origins were shifted off-plane.

not substantiated by an independent argument. In fact, a 2 Å shift leads to a  $\chi_{11}^{(1)}$  tensor component in good agreement with the charge field value whereas for  $\chi_{111}^{(2)}$ , it is a 1 Å shift.

In conclusion, the homogeneous dipole field approach, with a different dipole field for the anion and cation, is not suitable to describe the *in-crystal* environment on the isolated ion properties and therefore  $\chi^{(1)}$  and  $\chi^{(2)}$  of ionic organic crystals. Still, in some cases like DAST and DSTMS, the dipole field performs well when setting the origin at the barycenter of nuclear charges. However, in general, like for DAPSH, to get a good agreement with experiment and/or with the charge field approach, this origin must be shifted and there is no way to know beforehand the amplitude of this shift.

This research was supported in part by PL-Grid Infrastructure as well as by the Belgium government (IUAP No. P7/05, *Functional Supramolecular Systems*) and the Francqui Foundation. T.S. acknowledges the support from a Project operated within the Foundation for Polish Science MPD Programme co-financed by the EU European Regional Development Fund as well as the financial support from IUAP No. P7/05. The calculations were performed on the Technological Platform of High-Performance Computing of the Consortium des Equipements de Calcul Intensif, for which we gratefully acknowledge the financial support of the FNRS-FRFC (Convention Nos. 2.4.617.07.F and 2.5020.11), and of the University of Namur.

<sup>1</sup>T. Seidler, K. Stadnicka, and B. Champagne, *J. Chem. Phys.* **139**, 114105 (2013).

<sup>2</sup>T. Seidler, K. Stadnicka, and B. Champagne, *SPIE Organic Photonics + Electronics* (International Society for Optics and Photonics, 2013), p. 88270Y.

<sup>3</sup>T. Seidler, K. Stadnicka, and B. Champagne, *J. Chem. Phys.* **141**, 104109 (2014).